MANTECH Publications

Journal of Research in Physics and Applied Sciences
Volume 5, Issue 1, January-June 2022

A Study on a Bioactive and Antibacterial Nanocomposite

Dr. Shrikanth Muralidharan[1], Kajal Gupta[2]
Assistant Professor[1], Student[2]
Department of Physics
Hindustan Institute of Technology & Science
Corresponding Author's Email: - *shrimurali345@gmail.com[1]*

Abstract

Hydroxy-Apatite (HA) is commonly utilised as a bioceramic material because it exhibits chemical and mineral phases similar to human bone. Its biological characteristics enhance when it is replaced with metalions. Because of their increased surface area, HA nanopowders exhibit better sinterability and densification, as well as improved fracture toughness and other mechanical characteristics. When yttrium and cerium ions are added, it exhibits a high level of bioactivity and antibacterial activity. HA as a biopolymer with gelatin is more bioactive and changes sample particle nature. The hydrothermal process is a simple way to create this nanocomposite. The composition, crystallinity, and morphology of nanocomposite are investigated by FT-IR, XRD, and SEM-EDAX, respectively. In-Vitro bioactivity is evaluated by soaking in simulated bodily fluid for various days, and antibacterial activity is evaluated against prokaryotic microorganisms. Asfabricated nanocomposite is crystalline, with particles as small as 100nm, it is suitable for biomedical applications because to its bone bonding ability and antimicrobial properties.

Keywords: *Hydroxy-Apatite, Nanocomposite, Hydrothermal Method, Chemical and Mineral Phases*

INTRODUCTION

Bioceramics are now popular study subjects owing to their numerous orthopaedic uses, such as bone, tooth, bone tissue engineering, drug delivery applications, and so on. Because of its resemblance to bone, Hydroxy Apatite, Ca10(PO4)6(OH)2 is the most important

Page 43-49 © MANTECH PUBLICATIONS 2022. All Rights Reserved

bioceramic. Furthermore, hydroxyl-apatite may accept a wide range of additional mineral substituents to improve its mechanical and biological activities. Yttrium (Yt) is a vital mineral that promotes osteoblast growth while decreasing bone resorption. Despite being biocompatible, hydroxyl-Apatite lacks antibacterial activity, limiting its long-term stability and causing implant failures. The incorporation of antibacterial properties into HA is used to assure the success of the HA for biomedical applications. Cerium ions have long been utilised as antibacterial agents in medicine due to their great safety and broad spectrum of antibacterial action. Cerium-based bioceramic materials are gaining popularity because to their outstanding physical and chemical qualities, including great thermal stability, biocompatibility, and non-toxicity to human cells at low concentrations. Biopolymers such as Chitosan, Gelatin, and others are also employed to improve biological interactions with surrounding tissues. Gelatin, a natural polymer, is one of the known biopolymers that increases osteo-integration and promotes tissue regeneration. Furthermore, the inclusion of gelatin to the bioceramic increases not only the biological interactions, but also the mechanical characteristics of the biopolymer/bioceramic composite. The current study aims to synthesise a Gelatin/Ce,Yt-HA composite for biomedical applications using the major qualities of mineral ions like Yt and Ce substitution in HA and as a composite with gelatin for higher bioactivity and antibacterial property.

MATERIALS AND METHODS

Reactants: Analar Calcium Nitrate Tetrahydrate, Ca(NO3)2•4H2O; Yttrium Nitrate Hexahydrate, Yt(NO3)3.6H2O; CeriumNitrate Hexahydrate, Ce(NO3)3•6H2O; Diammonium Hydrogen Phosphate, (NH4)2HPO4; and Ammonium Hydroxide, NH4OH are starting materials.

Nanofacture: Analar grade Ca(NO)3.6H2O, Y(NO3)3.6H2O and Ce(NO3)3•6H2O are dissolved in deionized water. (NH4)2HPO4 is separately dissolved in deionized water. These two solutions were mixed in the molar ratio of 1.67. Then, gelatin solution is added in nitrogen atmosphere. Above reaction mixture is then stirred for 4h and pH 11 is maintained during synthesis. Precipitate so obtained is repeatedly washed with deionized water, filtered and then dried at 120°C for about 24h in hot air oven. Dried white powder is calcined

Page 43-49 © MANTECH PUBLICATIONS 2022. All Rights Reserved

and sintered in a muffle furnace for 3h. Nanocomposite so obtained Gelatin/ Ce,Yt/HA is used for characterization.

Nanocharacterization: Chemistry and Physical Metallurgy of nanocomposite is elucidated by FT-IR (Bruker, Tensor 27 Series) and XRD (Rigaku, Miniflex II). Structural Metallurgy and Morphology of as-synthesized composites is anlaysed with

SEM (JSM-6360LV, Jeol). The In-Vitro antimicrobial activity of as-synthesized composites is assessed against S.Aureus (gram+) and E.Coli (gram-) bacterial strains by well diffusion method. In-Vitro bone bonding ability is evaluated over as-synthesized composite by SBF test.

RESULTS AND DISCUSSION

FT-IR: Chemical composition of the Gelatin/Ce,Yt/ HA composite coating at different concentrations is carried out by FT-IR spectroscopy. IR spectra of the Gelatin/Ce, Yt-HA composite coating are shown in Fig.1 (Blue), which is found to be similar to that of Ce, Yt-HA. The characteristic peaks found in the spectra are attributed to the formation of Gelatin/ Ce,Yt-HA composite coating and no other peaks corresponding to any trace of impurities could be detected. Characteristics peaks obtained for Ce,Yt-HA composite coating is shown in Fig.1 (Brown). To account for them, the peaks appeared at 3441cm-1 and 1622cm-1 are due to the stretching and bending mode of adsorbed water, while the hydroxyl stretching peak for the composite is shifted to higher wave numbers at 3589cm-1.

The peak at around 3591cm-1 corresponds to the stretching mode of O-H group. The sharp peak at 1726cm-1 corresponds to the N-H peak in the Gelatin/Ce,Yt-HA composite. The peaks at 2924cm-1 and 2853cm-1 are attributed to the presence of C-H band in the gelatin present in the Gelatin/Ce,Yt-HA composite, which indicates that gelatin interacts with M-HA.

The carboxyl group of gelatin and composite is attributed to the at 1642cm-1. Hence, from the FT-IR results it is well supported that the formation of Gelatin/Ce,Yt-HA composite is favoured under all the coating conditions.

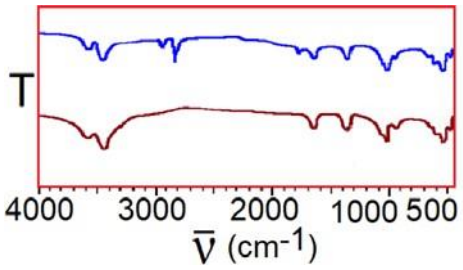


Figure 1: FT-IR spectra ofCe,Yt-HA (brown) and Gelatin/Ce,Yt-HA (blue).

Page 43-49 © MANTECH PUBLICATIONS 2022. All Rights Reserved

XRD: Pure Ce,Yt-HA and Gelatin Reinforced Ce,Yt-HA are similar to each other with an additional peak at ~26° is observed, which is ascribed to a graphite crystallographic (002) plane ofgelatin present in the Gelatin/Ce,Yt-HAP composite coating. These results are in good agreement with ICDD card No.41-1487. Fig.2 (Green) shows the XRD patterns for Ce,Yt-HA with peaks observed at 2θ values of 25.21°, 31.11°, 31.6°, 31.6°, 45.5°, 49.1° and 52.8°, respectively. The pattern found was similar to those that were obtained for Gelatin/Ce,Yt-HA shown in Fig.2 (Blue). Pattern of Gelatin/Ce,Yt-HA is in well agreement with the standard data for gelain/HA with the peak positions slightly shifted towards the lower angles from the standard patterns forgelatin/HA, indicating the substitution of Ce and Yt into the HA lattices. Thus, obtained XRD patterns support the formation Gelatin/Ce,Yt-HA nanocomposite.

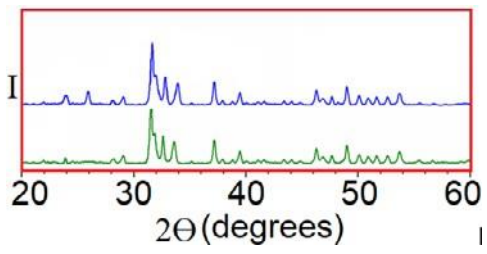


Figure 2: XRD patterns of Ce,Yt-HA (green) and Gelatin/Ce,Yt-HA (blue).

SEM-EDAX:Ce-HA, Ce,Yt-HA and gelatin/Ce,Yt-HA composite samples demonstrate that all the samples consist of spherical particles of different size and shape. The composite samples contain smaller spherical particles, some of which are arranged in clusters and others that are in a disordered arrangement. Spherical particles are observed in the Ce-HA and Yt-HA samples. The sphere shaped particles are not homogenously formed. Fine and compact morphology is observed in Gelatin/Yt, Ce-HA. In addition to that, the composite sample with spherical structures is found to possess few pores within them. The presence of pores in Gelatin/Ce,Yt-HA composite coating is beneficial for the initiation of bone formation, providing abundant site for the growth of osseous tissue. As the presence of Gelatin in the composite sample, the smaller spherical particles are arranged in cluster with other structural regularities. Based on the SEM examination, Gelatin/Ce,Yt-HA composite sample is found to optimum, which may pave the way for the better cell proliferation as shown in Fig.3 (Inset). EDX result of Gelatin/Ce,Yt-HA composite sample shown in Fig.3 shows that the sample is rich in Ca, Ce, Yt and P along with the presence of C. Thus, EDX analysis

Page 43-49 © MANTECH PUBLICATIONS 2022. All Rights Reserved

confirms the formation of Gelatin/Ce,Yt-HA composite on Ti.

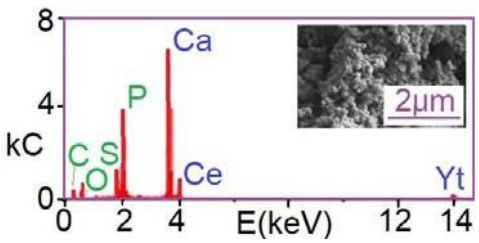


Figure 3: EDX analysis of Gelatin/Ce, Yt-HA with inset SEM image.

Antibacterial Active: The antibacterial activity of the Gelatin/Ce,Yt-HA composite is evaluated against the two bacterial strains by disc diffusion method. These two bacterial strains, E.Coli and S.Aureus, are model Gram- bacteria and Gram+ bacteria and are the general bacteria that are found in contaminated wounds.Zone of inhibition around different volume concentrations (25, 50, 75 and 100µL) of Gelatin/Ce,Yt-HA composite samples against E.Coli and S.Aureus. When comparing inhibition zone of HA coated samples against both bacterial strains, no appreciable antibacterial activity is seen which is clearly evident. The inhibition zones for E.Coli and S.Aureus are found to be 5 and 6mm for 25µL, 6 and 7mm for 50µL, 7 and 8mm for 75µL, 8 and 9mm for 100µL volumes, respectively. Apatite Crystal: As-synthesized Gelatin/Ce,Yt-HA composite samples are immersed in the freshly prepared SBF solution in order to test apatite crystal forming ability. Fig.4 shows the microstructure of the apatite growth on the Gelatin/Ce,Yt-HA composite at various period of immersion (viz., 1day, 7days, 14days, etc). Initiation of growth of apatite is found on HA coating after 1day of immersion in SBF solution, which can be well evident from Fig.4 (Left). The magnified image of this figure (inset) displays the formation of apatite on the sample. Small spongy like apatite growth on the gelatin/ Ce,Yt-HAP at 7 days of immersion (micrograph not shown). The mixed type of spongy and feather-like apatite on the Gelatin/Ce,Yt-HA grows on increasing the immersion period upto 14days shown in Fig.4 (Right). The obtained results reveal that the process of apatite formation can take place through Kim mechanism.

Accordingly, apatite formation of the sample takes place through a sequence of chemical reactions. Thus, the micrographs display the apatite mineralization ability at 1day and 14 days of immersion, revealing that the resultant gelatin/Ce,Yt-HA composite sample with improved bioactivity in SBF solution.

Page 43-49 © MANTECH PUBLICATIONS 2022. All Rights Reserved

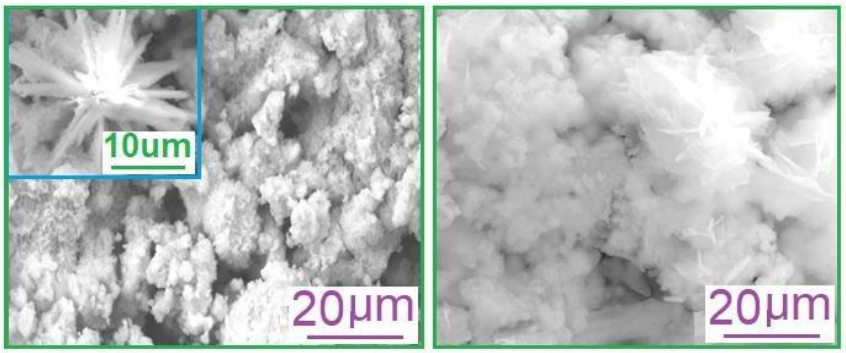


Figure 4: Apatite crystals after a day (left), and after 14 days (right) of immersion in SBF.

CONCLUSION

A new antibacterial and bioactive Gelatin/Ce,Yt-HA composite that may be employed for a variety of biological applications has been successfully produced. The development of Ce,Yt-HA and Gelatin/Ce,Yt-HA nanocomposite is supported by structural characterisation investigations.

Morphological findings show that the substituent's are dispersed evenly and discretely. It is well established from antibacterial activity tests against E.Coli and S.Aureus that the addition of Ce increases the anti-bacterial activity of nanocomposite. Furthermore, the Gelatin/Ce,Yt-HA composite has superior bone bonding potential, highlighting the bioactive character of the composite. Thus, the Gelatin/Ce,Yt-HA composite achieves an excellent balance of antibacterial properties. As a result, these synthetic composite materials are a very attractive option with a better knowledge of cell/biomaterial interactions, and they will find wide applications in the fields of Orthopedics (Bone) and Dentistry (Tooth).

REFERENCES

1. M.Nikoo, X.Xu, S.Benjakul, G.Xu, J.C.R.Suarez, A.Ehsani, L.M.Kasankala, X.Duan, S.Abbas (2011), "Characterization of gelatin from the skin of farmed Amur sturgeon Acipenserschrenckii", International Aquatic Research, Volume 3, pp. 135−145.
2. F. V. Anghelina, D. N. Ungureanu , V. Bratu, I. N. Popescu, C. O. Rusanescu (2013), "Fine structure analysis of biocompatible ceramic materials based hydroxyapatite and metallic biomaterials 316L", Applied

Page 43-49 © MANTECH PUBLICATIONS 2022. All Rights Reserved

Surface Science, Volume 285, pp.65−71.

3. C. T. Laurencin, A. M. A. Ambrosio, M. D. Borden, J.A.Cooper (1999), "Tissue Engineering: Orthopedic Applications", Annual Reviews of Biomedical Engineering, Volume 1, pp.19−46.
4. O. Kaygili, S. V. Dorozhkin, T.Ates, N. C. Gursoy, S. Keser, F. Yakuphanoglu, A. B. Selcuk (2015), "Structural and dielectric properties of yttrium-substituted hydroxyapatites", Material Science and Engineering C, Volume 47, pp.333−338.
5. J.H.Muyonga, C.G.B.Cole, K. G. Duodu (2004), "Fourier Transform Infrared (FTIR) Spectroscopic study of acid soluble collagen and gelatin from skins and bones of young and adult nile perch (Lates niloticus)", Food Chemistry, Volume 86, pp.325−333.
6. T.Nguyen, B.Lee (2010), "Fabrication and characterization of cross-linked gelatin electrospunnanofibers", Journal of Biomedical Science and Engineering, Volume 3, pp.1117−1124.
7. J. Ratanavaraporn, S. Damrongsakkul, N. Sanchvanakit,T. Banaprasert, S. Kanokpanont (2006), "Comparison of gelatin and collagen scaffolds for fibroblast cell culture", Journal of Metals, Materials and Minerals, Volume 16, pp. 31−36.
8. T.Nguyen, B.Lee (2010), "Fabrication and characterization of cross-linked gelatin electrospunnano fibers", Journal of Biomedical Science and Engineering, Volume 3, pp.1117−1124.
9. J.S.Mao, L.G.Zhao, Y.J.Yin, K.D.Yao (2003), "Structure and properties of bilayer Chitosan–Gelatin scaffolds", Biomaterials, Volume 24, pp.1067– 1074.
10. F.V.Anghelina, D.N.Ungureanu, V.Bratu, I.N.Popescu, C.O.Rusanescu (2013), "Fine structure analysis of biocompatible ceramic materials based hydroxyapatite and metallic biomaterials 316L", Applied Surface Science, Volume 285, pp.65−71.

Page 43-49 © MANTECH PUBLICATIONS 2022. All Rights Reserved